Lykilsíða

Skýrsla nr.	Dags.	ISSN	Opin ☒ Lokuð ☐
VÍ 2018-019	Desember 2018	1670-8261	**Skilmálar:**

Heiti skýrslu / Aðal- og undirtitill: Vinna við kvörðun WaSIM líkans á vatnasviðum með ríkan grunnvatnsþátt	**Upplag:** **Fjöldi síðna:** 33
	Framkvæmdastjóri sviðs: Jórunn Harðardóttir
Höfundar: Morgane Priet-Mahéo, Andréa-Giorgio Massad, Sif Pétursdóttir, Davíð Egilson, Matthew James Roberts	**Verkefnisstjóri:** Davíð Egilson
	Verknúmer: 4314-0-0002
Gerð skýrslu/verkstig:	**Málsnúmer:** 2018-226 / 2019-0370

Unnið fyrir: Landsvirkjun – GEFUR ÚT
Samvinnuaðilar:

Útdráttur:

Vatnafræðilega líkanið WaSIM var notað til líkja eftir rennsli Ytri Rangár. Það er hluti af tilraunaverkefni til að kanna hvort líkanið henti til að herma rennsli vatnsfalla sem hafa ríkan grunnvatnsþátt. Rennslismælingar hófust í Ytri Rangá árið 1961 en samfelldar stafrænar mælingar sem notaðar voru við líkangerðina eru til frá 2004. Það var talsverð áskorun að líkja eftir rennslinu því lykillin er nokkuð óstöðugur vegna reks gosösku frá Heklu eftir farveginum. Lögð var áhersla á einfaldleika í uppsetningu á líkaninu og 14 breytur voru valdar til kvörðunar. Sannprófun líkansins sýnir að unnt er að að herma rennsli lindáa með WaSIM með góðri samsvörun en ekki síður að líkangerðin getur aukið skilning á mæligögnunum og bætt kvörðun á rennslislyklinum. Eftir stendur að vinna þarf betur úr grunnvatnsþættinum sjálfum og er stefnt að því í tengslum við verkefni komandi árs.

Lykilorð: WaSiM, vatnasvið, grunnvatn, sjálfvirk bestun á inntaksbreytum, Ytri Rangá, grunnvatnslíkan	**Undirskrift framkvæmdastjóra sviðs:**
	Undirskrift verkefnisstjóra:
	Yfirfarið af:

Table of Contents

1 Introduction

Iceland's freshwater is an important resource for the country providing drinking water and energy. Groundwaters represent about 20% of the country's freshwater (Sigurðsson, 1992) and are the subaerial source for many freshwater rivers and lakes. During the past 60 years, many rivers have been monitored by Icelandic institutes such as Vatnamælingar, Orkustofnun, Landsvirkjun and Veðurstofa Íslands, providing good local knowledge of the monitored catchments. However, these measurements are restricted in space and provide limited information on what is happening higher in the catchments. Hydrological models have been developed to bridge that knowledge-gap and they can be used for estimates when measurements are unavailable.

At IMO, the hydrological model WaSiM has been used for about a decade now and it has been used in Iceland for hydropower potential assessment projects and flood prediction models. The model performs well in catchments where the discharge is mainly resulting from direct run-off, and contributions from glaciers and lakes have been successfully included in the model. However, groundwater contribution has been more difficult to incorporate (Einarsson & Jónsson, 2010), and catchments with significant groundwater contributions have, until now, been omitted from analysis.

In this research project, the hydrological model WaSiM is tested on the Ytri Rangá catchment – a catchment with substantial groundwater contribution in southern Iceland. Geographical and geological conditions affect waterflow through the catchment, and this is described in the following section, in addition to an overview of previous discharge measurements in Ytri Rangá. In the third section, the methodology is presented, including the calibration steps and the automatic optimization method used in the simulations. The results of the best model setup are investigated, and the performance of the model is discussed. Finally, the results of the hydropower-potential assessment are presented.

2 Ytri Rangá, Árbæjarfoss

2.1 Description of the catchment

Ytri Rangá is located in the South Icelandic Volcanic Zone (SIVZ), it takes its source at Valafell and flows down through the town of Hella. The catchment is approximately 622 km^2; it is elongated (57 km long, 13 km wide) and located at a mean elevation of 365 m above sea level. River discharge is measured at station vhm 59, north of Hella (Figure 1 and Figure 2). Within 2 km from the outline of the catchment of Ytri Rangá there are 46 boreholes, two of them are research boreholes at Lækjarbotnar (Figure 2).

The catchment includes the north west flank of Hekla and the volcano has been shaping the catchment with its lava flows and ash depositions. Consequently, the bedrock in the catchment is recent and it is composed mostly of lava flows, although palagonite (móberg) is also present (Figure 1). Surface faults and volcanic fissures occur in the basin, with SW-NE orientated fissures in the east of the catchment due to volcanism and N-S trending faults in the east a product of large earthquakes. These tectonic features allow for vertical exchange of water between the surface and aquifers.

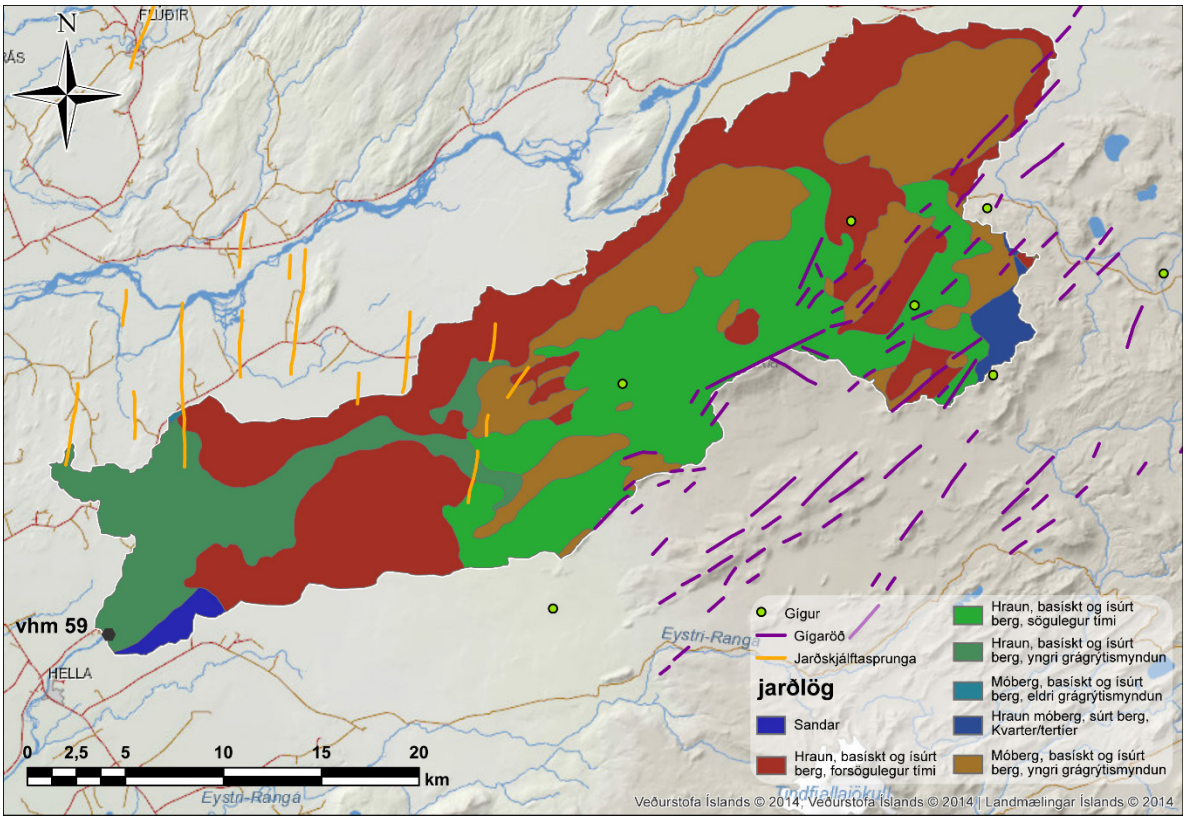

Figure 1. Geology of the Ytri Rangá catchment (source: Náttúrufræðistofnun Íslands).

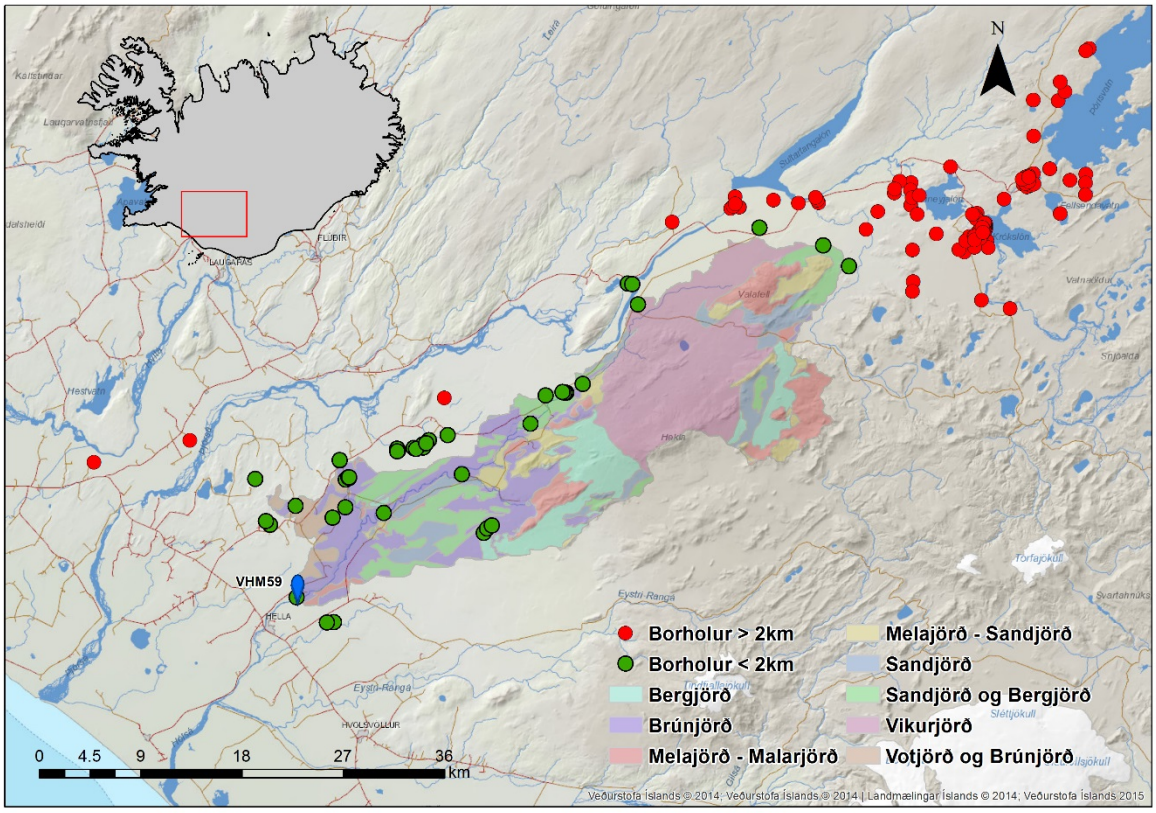

Figure 2. Catchment of Ytri Rangá: soils and measurement stations.

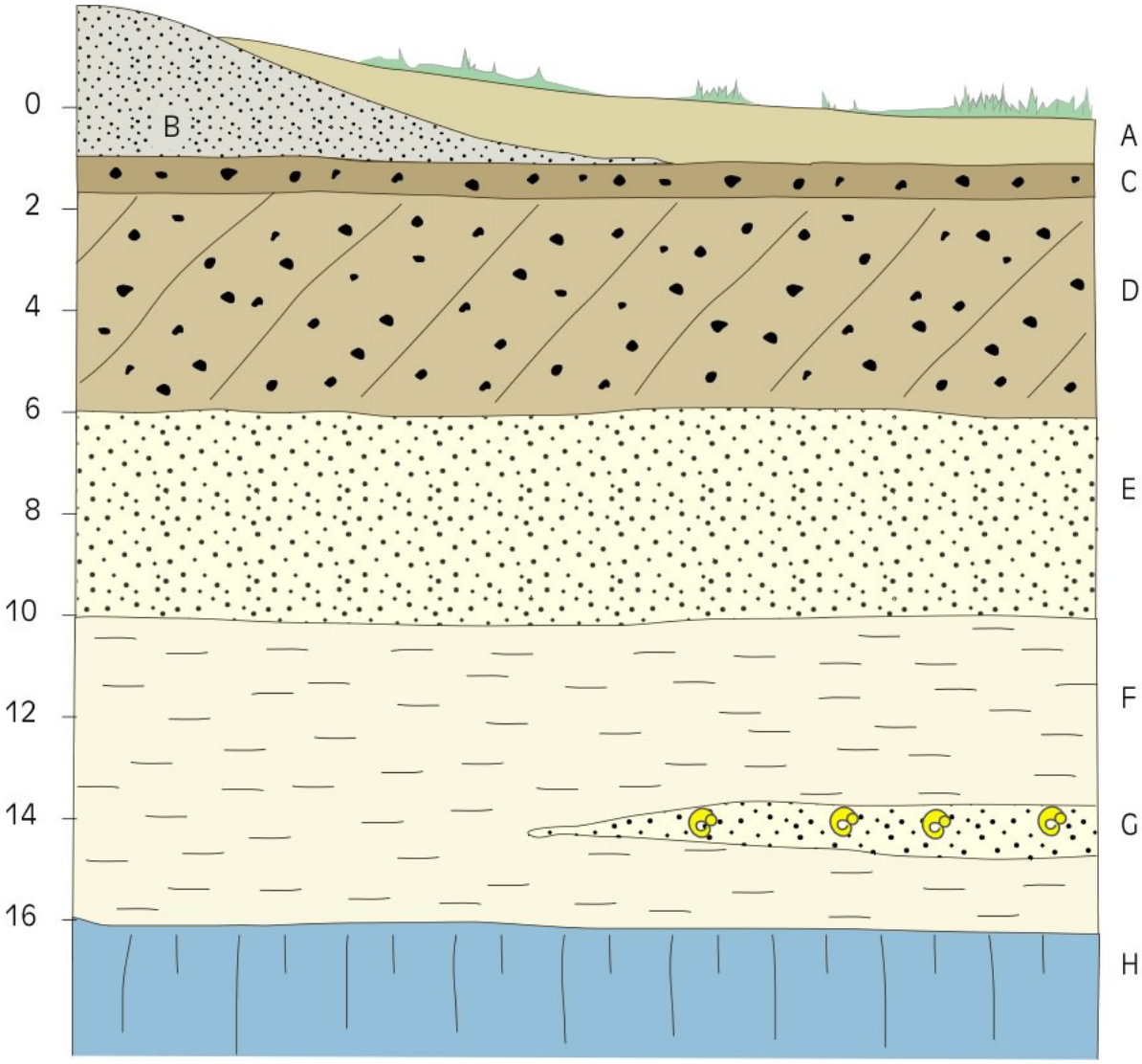

Figure 3. Stratigraphic column at Ytri Rangá. A) soil, B) aeolian sand, C) horizontally stratified gravel deposit, D) cross-stratified gravel and sand, glaciofluvial delta deposit, E) stratified to laminated silty sand, marine pro-delta sediments, F) laminated silt and fine sand, glaciomarine sediment, G) fine to coarse sand with shells, H) Bedrock, tertiary basaltic bedrock with intercalated sediments (source (Hjartarson & Ingólfsson, 1988)) (Hjartarson, 2005).

The soils in the catchment (Figure 2) are mainly volcanic (andosols) in origin (eldfjallajörð) (Arnalds & Óskarsson, 2009) and, being highly porous, they can accommodate high amounts of water. A larger part of these soils are vitric/glerjörð (melajörð, malarjörð, sandjörð og vikurjörð) but sortujörð is also present (brúnjörð og votjörð). Pores in andosols are mostly large or intermediate, therefore allowing for rapid water transport and rapid water infiltration in addition to both saturated and unsaturated hydraulic conductivity compared to most other soils (Arnalds, 2015). Bergjörð is also observed in the catchment over lava formed during historical times (Figure 1).

Figure 3 is a sketch of a stratigraphic column located in proximity to Ytri Rangá and shows a 16 meter deep soil mostly composed of sands with high permeability values ranging from 10^{-3}-10^{-4} for the top layer to 10^{-7} m/s for the bottom layer (Hjartarson, 2005). The bedrock is

expected to have a similar level of permeability (Hjartarson, 1994) but fractures are increasing the permeability significantly locally, causing anisotropy i.e. directional flow mainly along direction of the fractures.

2.2 Water level station vhm 59

Gauging station vhm 59 is located on the right bank of Ytri Rangá and has been recording the discharge of Ytri Rangá since October 1st, 1961. The station was setup originally due to the interesting hydropower potential opportunities of this large spring river, it has also been used to monitor the state of the groundwater resources and assess the effect of the regulation of Þjórsá on the catchment. In September 2004, the gauge which was recording daily water level on paper was replaced by an electronic instrument providing digital measurements at least on hourly basis.

2.2.1 Statistical analysis of the discharge measurements

From gauging measurements (Veðurstofa Íslands, 2015) , the average discharge over the time period 1961–2015 is 44.7 m^3/s. The maximum yearly-averaged value was reached in hydrological year 1991/1992 with 57.1 m^3/s and the minimum yearly-averaged value reached in 1978/1979 with 36.0 m^3/s. The largest instantaneous discharge was measured on Feb. 27th, 1968 with about 500 m^3/s and the smallest instantaneous discharge was measured on May 21St, 1979 with 28.3 m^3/s.

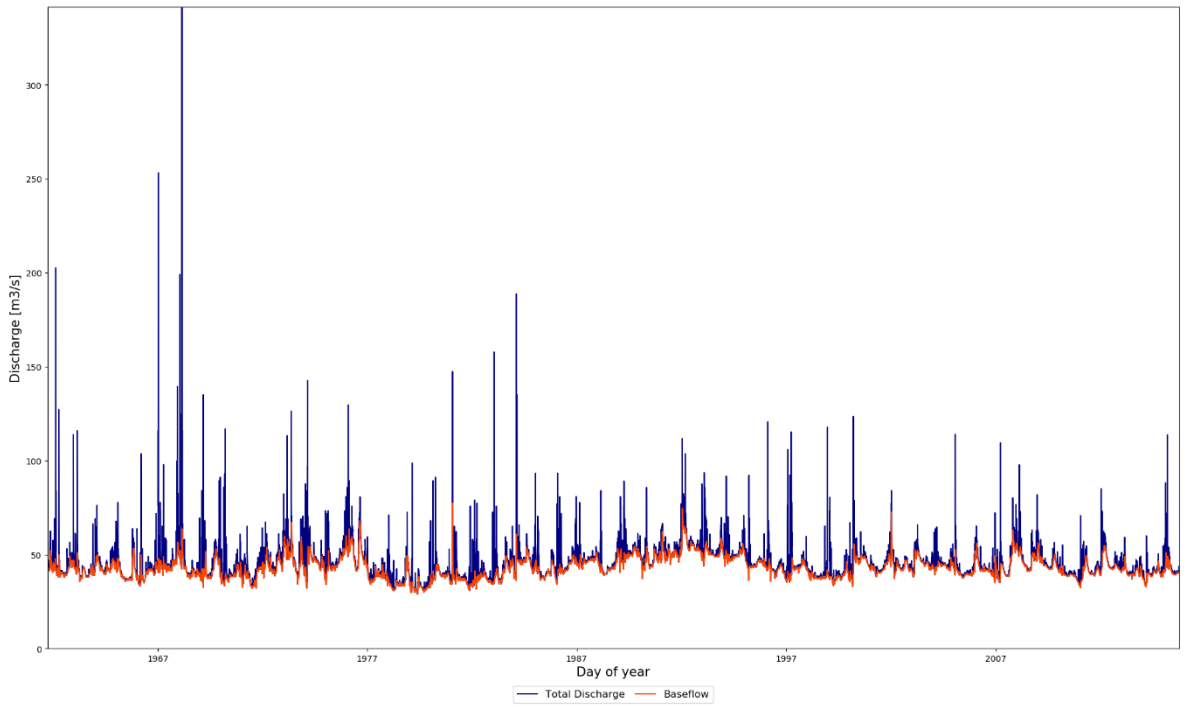

Figure 4. Daily averaged discharge (blue line) and baseflow (red line) as computed by the HYSEP local minimum method with a 5 days window for station VHM 59 from Oct.1st, 1961 to Sep.30th, 2015.

Figure 4 shows the daily-averaged discharge (in blue) from 1961 to 2015 as a continuous timeseries covering 53 hydrological years in total. Baseflow was computed at five-day intervals using the local-minimum method of hydrograph separation from the USGS software HYSEP (Sloto & Crouse, 1996) with a 5 days interval is also shown in red in Figure 4.

The interannual variability can be studied from Figure 5, Figure 6 and Table 1. Figure 5 displays the total discharge (in blue) averaged for each day of the year over the whole timeseries and baseflow (in red) calculated as described for Figure 4. Only slight variations are apparent over the year with a baseflow relatively constant at a mean value of 44 m^3/s and daily averaged discharge varying between 41 and 54 m^3/s. During the summer months, the baseflow accounts for most of the total discharge while in winter months, the total discharge varies more as the ground freezes and surface runoff feeds the river directly.

Table 1. Maximum, mean and minimum discharge for each month of year for station VHM 59 from 1961 to 2015.

	Jan	Feb	Mar	Apr	May	Jun	Jul	Agu	Sep	Oct	Nov	Dec
Max	253.19	341.33	135.19	127.33	126.41	59.86	62.2	80.73	68.08	80.28	72.65	139.52
Mean	46.42	47.6	46.41	44.76	43.06	42.26	42.13	42.89	44.03	45.03	45.71	46.03
Min	30.83	29.98	30.83	29.98	29.13	32.22	32.22	30.83	29.98	30.83	30.83	32.6

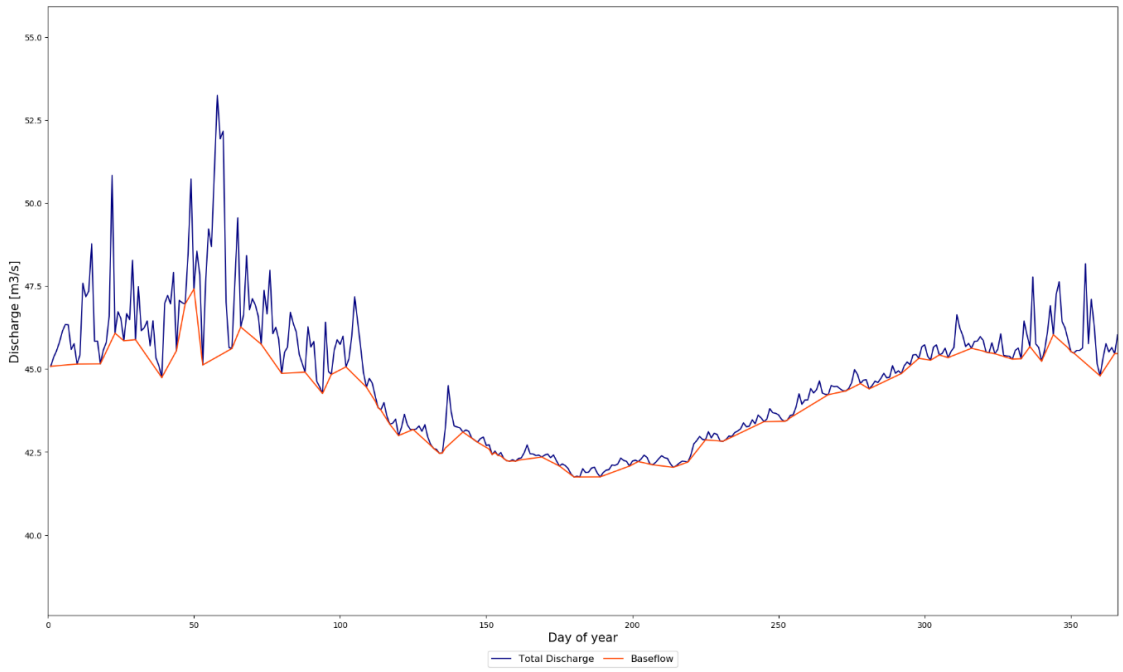

Figure 5. Discharge (blue line) averaged for each day of year over the whole time period and baseflow (red line) as computed by the HYSEP local minimum method with a 5 days window.

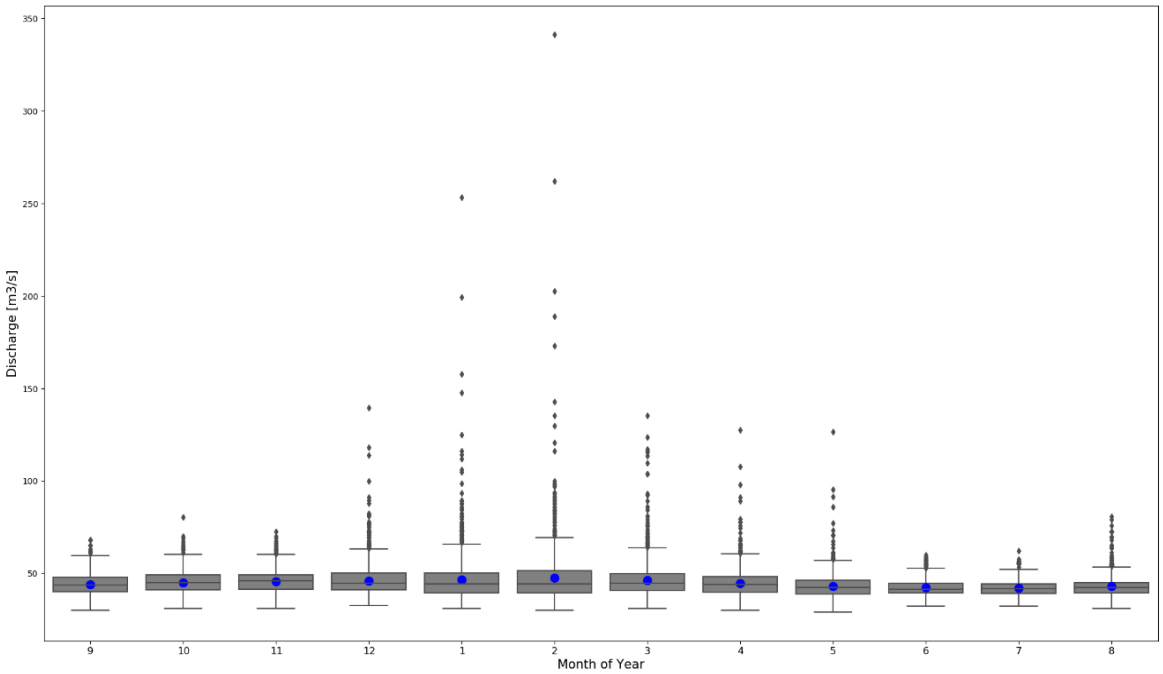

Figure 6. Boxplot for each month of year from daily discharge recorded over hydrological years (October 1962 – September 2014) at station vhm59. Blue dots show the mean value for each month over the same period.

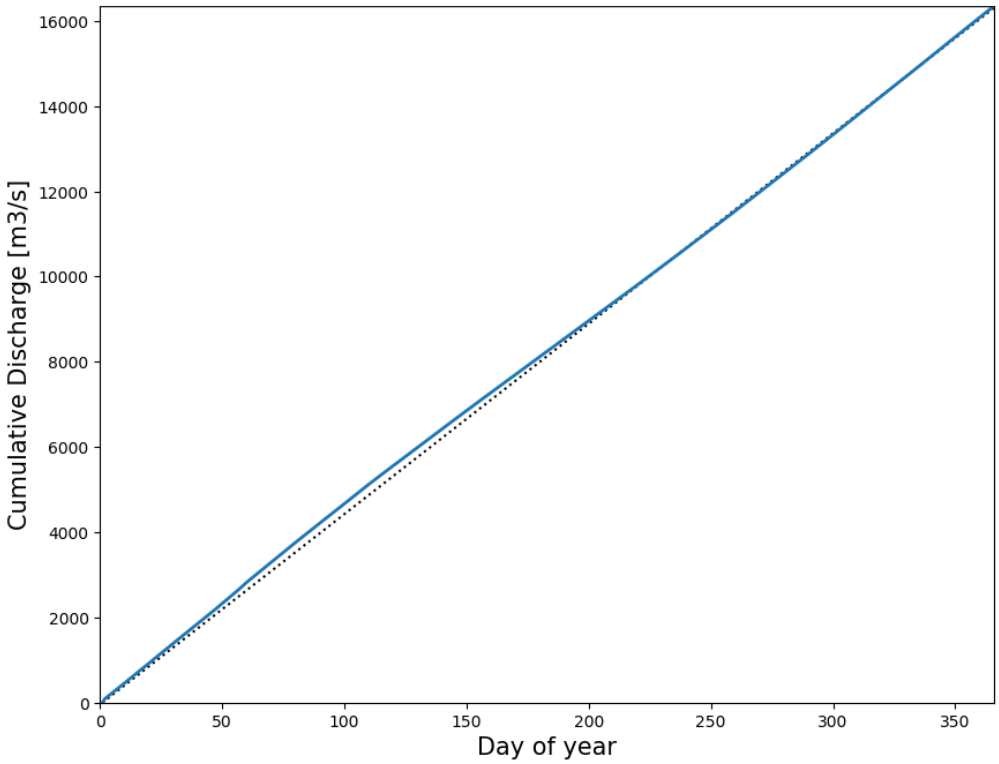

Figure 7. Mass curve (blue line) over period 1961–2015 for station VHM 59 with the constant discharge reference line (black dotted line).

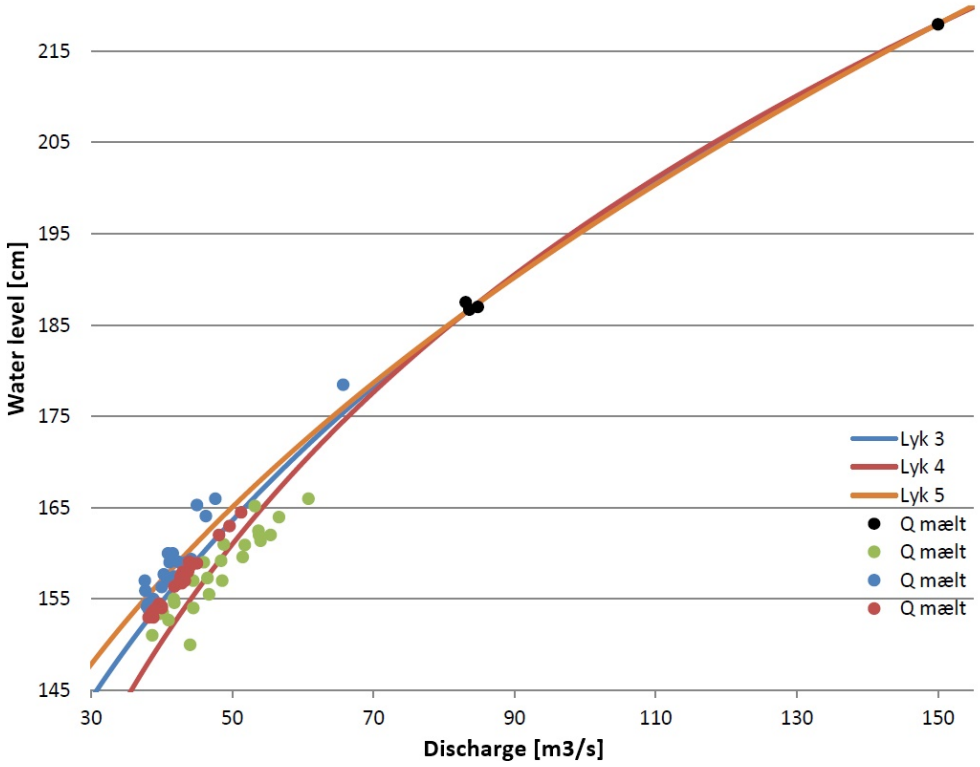

Figure 8. Stage curves 3, 4 and 5 for station vhm 59, V321 at Ytri Rangá, Árbœjarfoss along with the 76 measurements used for the definition of curve n. 3 (all points) , the peak flow measurements defined as forcepoints (black points), measurements used for the definition of stage curve n. 4 (green and black points) and curve n.5 (blue and black points) (Image from (Reynisson, 2015)).

The relative steadiness of the discharge over the year can be further illustrated by Figure 6 which shows boxplots for each month of the year calculated from the daily discharge over the whole timespan. Maxima are reached in January and February which correspond to the colder months, when the surface is frozen. Those results can also be read on Table 1 which presents the maximum, minimum and mean averaged discharge over the 54-year timespan. Maxima are reached in the winter months while mean and minimum values remain constant throughout the year.

In Figure 7, the mass curve follows closely the dotted line which represents the mass curve of a catchment with constant flow rate. This is typical of groundwater-fed rivers as their daily cumulated discharge increases relatively consistent with each day of the year (Gröndal, 2004; Stefánsdóttir & Egilson, 2014). A previous analysis of the master recession curve for discharge measured at station vhm 59 (Lugten, 2013) supported that the seasonal differences of the discharge are small, it shows that the catchment has a high $Q25/P_{discharge}$ coefficient (1.16 m^3/s) indicating that the baseflow component is high.

2.2.2 Stage-discharge curves

Volcanic deposits from previous Hekla eruptions sit unevenly in the river bed and, as they resuspend and get <transported further, they can affect stage-discharge estimates. Five stage curves were made to fit the measurements performed since 1961 to attempt to account for these dynamic changes of the river bed (Reynisson, 2015). Nowadays the three last stage curves (nr. 3 to 5) are used over the period from 1961 to 2015 in order to rectify the discharge computation.

Figure 8 illustrates how difficult it is to obtain a single rating curve that would satisfy the field measurements, as water levels can be associated to discharges differing by up to 15 m^3/s. Looking in details the months during which the control measurements were performed, it appears that the blue outliers were mostly measured during late summer-fall (end of July to November) while the green outliers were almost all obtained in May-June. This suggests that the rating curves will tend to underestimate the discharge in spring time, early summer while it will tend to overestimate it at the end of the summer and fall time.

3 Methodology

The grid-based water flow and balance simulation model (WaSiM) was used to simulate the discharge in the catchment (Schulla, 2017). The model used gridded terrain data with 1x1 km grid size. Meteorological data were taken from the reanalysed results of the HARMONIE numerical weather prediction model (Bengtsson, o.fl., 2017) These data were resampled from a 2.5x2.5 km grid to the 1x1 km grid used by WaSiM. To simplify the hydrological model, and given that the simulation timestep is 24h, the model only uses air temperature and precipitation as weather inputs.

The WaSiM model is composed of modules that allow some adaptability to the diversity of existing catchments. Good experience has been acquired at IMO with this model to simulate discharge in catchment with direct runoff, lake, glacier and little groundwater recharge. However, basins with large contribution from groundwater have been up to now set to the side due to the complexity of the setup and calibration process. Einarsson and Jónsson (2010) showed that the activation of the groundwater module improves significantly the discharge computation, however simulations with two aquifers resulted in errors and artificially increased discharge.

Simple setups are always favoured against complex setup in particular when the added parameters are unknown and result from experimental calibration. Preliminary tests were performed to investigate the importance of parameters for the quality of results: number of aquifers, groundwater storage coefficient, groundwater level, recession parameters k for base discharge, number of soil layers, boundary conditions (bh and bq) and leakage factor (gk) between aquifers were all investigated to assess the model sensitivity to their change. In addition to the unsatzon module, groundwater and soil module were turned on. Spring water is expected to emerge at the northern end of the catchment, the amount though is left to calibration but is estimated to be between 2 and 48 m^3/s.

The simulations for the calibration are performed over hydrological years 2005 to 2014, but three years are used as warming up time for the model. Results are therefore considered from September 2008 and August 2015.

The validation was performed over hydrological years 2004 to 2016, the three first years being used for initiating the model. The results should be considered with a critical eye as the discharge data is unchecked for hydrological years 2015 and 2016. During cold weather, the gauge might be affected by ice, resulting in imprecise readings.

3.1 Calibration of the model

Calibration consists in testing parameters whose value is uncertain in order to obtain good results. 14 parameters were retained for calibration (CWH, param_kelsqd_1_summer, snowmelt_coeff, drainage, krec, conductivity, mult, colmation, slayers, bq, clayperm, c1_coeff, T0, dT) that are related to the terrain properties and the formation and melt of snow in the model.

3.1.1 Error measures

To assess the quality of the results, several measures of the error are used on the whole dataset or on subsets : the mean error (ME), the root mean square error (RMSE), the efficiency coefficient both on the raw data (NS) and on the logarithm of the observed and simulated data (log-NS) (Krause, Boyle, & Bäse, 2005) and finally the average snowpack on the 31st of August, at the end of the hydrological year (Table 2). A specific focus is set on the efficiency coefficients which are easier to interpret than RMSE and ME. In addition, the simulation period was divided into period of interest – winter (September-March) and spring (April-August) – and maxima, daily and yearly averages were computed.

A combination of these measures is used to attempt to account for more considerations in one criterion: the score criterion is a relative measure of the performance of the model and is computed such as:

$$score = 0.35RK_{NS_{Q_{all}}} + 0.15RK_{log-NS_{Q_{all}}} + 0.1RK_{RMSE_{Q_{year}}} + 0.3RK_{NS_{\bar{Q}_{daily}}} + 0.1RK_{logNS_{\bar{Q}_{daily}}}$$

Where RK is the value within the linear sequence from 0 to 1 and of size n associated to the same sorting position than the error measure rank within the set of n simulations. Hence, for a set of three simulations, getting respectively 0.3, 0.29, 0.6 for NS_{Qall}, $RK_{NS_{Q_{all}}}$ would be respectively 0.5, 0 and 1.

Table 2. Error measures, with O and P respectively the observed and predicted values.

Mean error	$ME = \frac{1}{n}\sum_{i=1}^{n} P_i - O_i$
Root mean square error	$RMSE = \sqrt{\overline{(P_i - O_i)^2}}$
Nash-Sutcliffe efficiency	$NS = 1 - \frac{\sum_{i=1}^{n}(P_i - O_i)^2}{\sum_{i=1}^{n}(O_i - \bar{O})^2}$
Nash-Sutcliffe efficiency with logarithmic value	$log - NS = 1 - \frac{\sum_{i=1}^{n}(\log(P_i) - \log(O_i))^2}{\sum_{i=1}^{n}(\log(O_i) - \overline{\log(O)})^2}$

3.1.2 Automatic parameter calibration using Adaptative Simulated Annealing (ASA)

In order to predict floods or to reconstruct historical discharge time series, hydrologists are more and more relying on hydrological models. Hydrological models are complex and need to be adapted and calibrated for each catchment studied, multiple parameters have to be tuned in order to obtained reliable results. However, many of the parameters cannot be directly obtained through measurements or prior information and, as the modification of a parameter can affect the next one, manual calibration can sometimes turn out to be an arduous and long task (Arsenault, Poulin, Côté, & Brissette, 2013).

Automatic calibration can be performed through the implementation of optimization algorithms, many studies have shown that they lighten the work of the modeler (manhours) (Seibert, 2000) and most often improve the results of the models (Efstratiadis & Koutsoyiannis, 2010). Two aspects are considered when selecting an algorithm, its ability at finding global optimum and its computing performance (how fast it will find that optimum).

The Simulated Annealing algorithm (SA) or its faster variant the Adaptative Simulated Annealing (ASA) have been pointed out by numerous article as a performant optimization algorithm, able to find global optimum in relatively short time (Arsenault, Poulin, Côté, & Brissette, 2013; Goswami & O'Connor, 2007). This algorithm is well documented and has been tested within models in lots of diverse field including hydrology (Ingber, 1996).

The ASA algorithm was implemented within WaSiM hydrological model in order to automatize and improve the calibration procedure. Pyasa is a Cython based bindings for Lester Ingber's Adaptive Simulated Annealing developed by Robert Jördens, it is used to create a python interface linking the WaSiM model and the algorithm. A range is predefined for each parameter being calibrated and the algorithm is set up look for the global minimum using $1\text{-}NSE_{Qall}$ hence aiming at finding the highest NSE_{Qall} as possible.

3.2 Hydropower potential assessment

Once a model is calibrated and validated, the results can be used to estimate the discharge within the catchment. For that purpose, sub-catchments are selected by the definition of extra pour points along the main stream (Figure 9) at which discharge will be recorded. This aspect will be further developed next year together with the outcome of VHM 116.

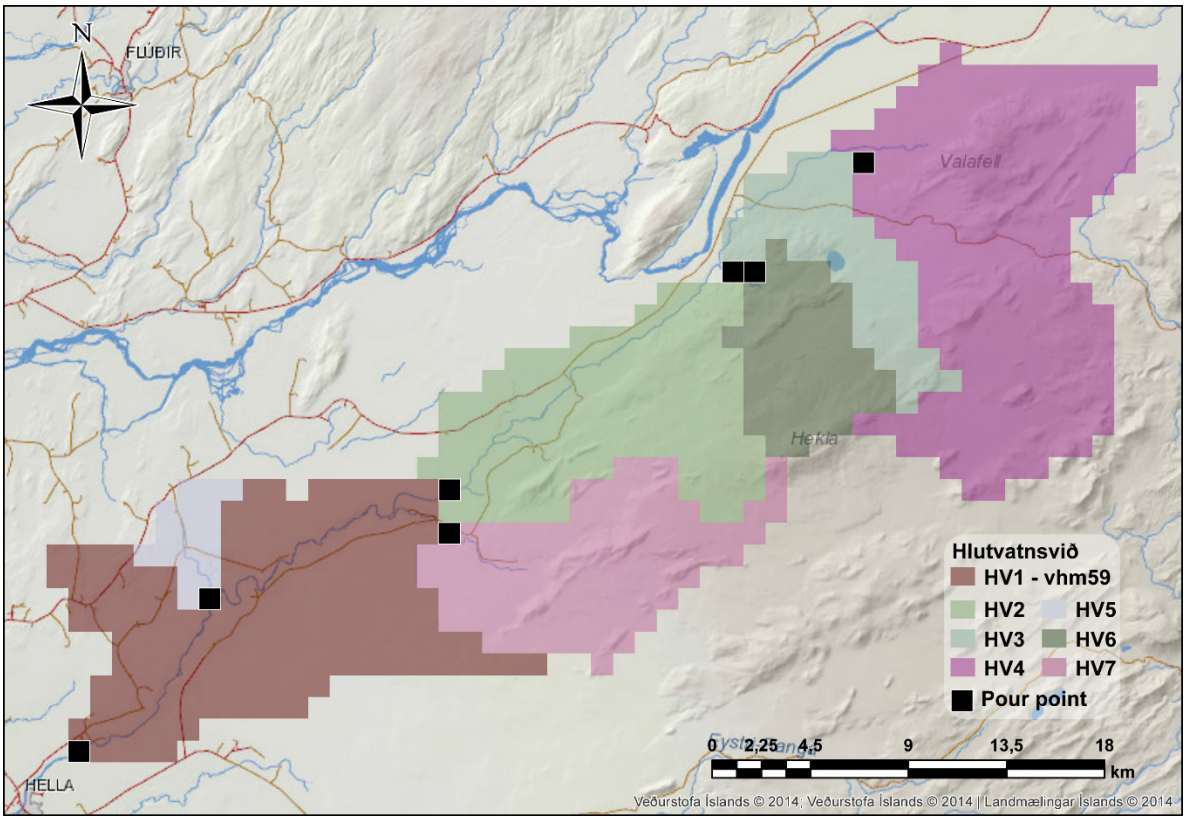

Figure 9. Delineation of the sub-catchments as defined in WaSiM, each sub-catchment area is represented by a color and their pour point is marked by a black square.

4 The model runs

4.1 Model calibration

The model ran over 20000 times with a semi-randomized parametrization approach and over 300 times with a manual approach. These simulations allowed us to investigate the modules and find which parameters have the most influence on the results as well as the best description of the terrain (14 different alternative GIS setup were tested). Best results were obtained with the use of a single aquifer.

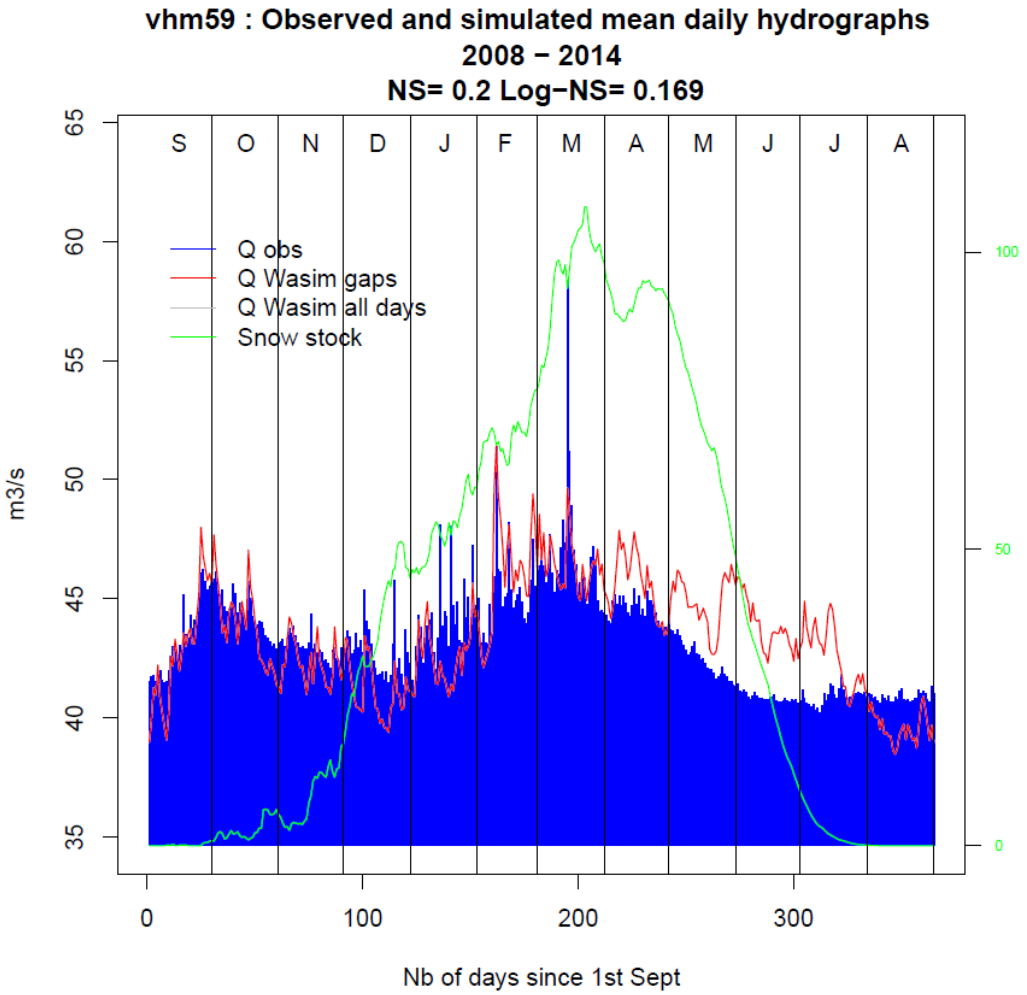

Figure 10. Mean daily discharge for the best run for the semi-automatic and manual calibration process.

While these test runs provided good insights on the most successful setup and parameters to calibrate, they did not lead to satisfactory results. The best run of the last test set is presented in Figure 10 :while the Nash-Sutcliffe value for the daily mean discharge is 0.2, this value falls to less than 0.1 when the simulation results are compared with the measurements on the daily basis (NS_{Qall}), which suggests that the model performed just slightly better than the statistical mean. Looking at Figure 10, we observed that the winter estimates are overall better than the summer estimates, but it still tends to underestimate the discharge. The spring peak is greatly underestimated, and the spring/early summer discharge is overestimated by almost 5 m^3/s while the discharge during the high summer is rather underestimated.

Because of the poor performance of the semi-automatic and manual calibrations, a new calibration approach was developed, and ASA automatic optimization was used on the catchment. The model was run more than 16900 times in automatic optimization mode. This method quickly obtained better results than the semi-automatic calibration: NS_{Qall} exceeded 0.4 within 100 runs. The results are evaluated using different statistical measures described in the methodology, in addition to the score criterion and the efficiency coefficient of the data set (NS_{Qall}), three other error measures were also considered to set focus on different aspects of the discharge such as high peak flows, seasonal trends and the spring season. The simulations scoring highest for these five criteria are presented in Table 3.

Table 3. Performance of the best calibration runs. The runs selected rank highest according to five reference error measures and are named after them. The values used in the computation of the score criterion are emphasized in bold in the table.

	score	**NS_{Qall}**	**NS_{Qmax}**	**NS_{Qmean}**	**$NS_{Qspring}$**
ME_{all}	0.03	0.15	1.98	0.02	-0.02
$RMSE_{all}$	3.71	3.68	5.60	4.02	4.21
NS_{Qall}	**0.599**	**0.604**	**0.083**	**0.528**	**0.482**
Log-NS_{Qall}	0.596	0.611	0.103	0.510	0.457
ME_{Qyear}	-0.008	0.084	2.243	0.070	-0.132
$RMSE_{Qyear}$	**1.65**	**1.48**	**3.29**	**1.84**	**1.92**
NS_{Qyear}	0.561	0.645	-0.749	0.450	0.407
ME_{Qmax}	-15.00	-15.08	-0.08	-12.26	-16.71
$RMSE_{Qmax}$	20.1	19.4	8.1	17.7	20.4
NS_{Qmax}	**-0.138**	**-0.060**	**0.813**	**0.117**	**-0.178**
$ME_{Qspring}$	2.029	1.353	7.246	3.427	0.321
$RMSE_{Qspring}$	3.59	3.05	8.73	4.85	1.92
$NS_{Qspring}$	**0.516**	**0.649**	**-1.870**	**0.114**	**0.862**
NS_{Qmean}	**0.613**	**0.495**	**-0.883**	**0.647**	**0.182**
Log-NS_{Qmean}	0.621	0.496	-0.782	0.654	0.149
$snowstock_{end}$	22.27	30.42	0.26	22.30	0.64

Examining the results from the best selected simulations (Table 3), we observe that the simulations (with the exception of simulation NS_{Qmax}) obtain good results for most error measures. However, it appears that runs with higher NS_{Qall} are also associated with increased snow stock at the end of the hydrological year. The maximum peak discharge is also generally poorly estimated.

Figure 11 presents the general performance of the model over the hydrological years 2008-2014 for the best score criterion, similar figures are provided in 0 for the other selected runs. It shows that the discharge is overall well simulated but fall and winter flow tend to be slightly underestimated while on the other hand, the late spring-summer flow are overestimated, resulting possibly from the too large snow pack accumulated during the winter season. This is though in good agreement with the notion that the rating curves tend to underestimate spring discharge while overestimating late summer-fall discharge.

The calibration shows some variability in the performance of the simulation: within the hydrological year with the discharge of June to August (months of low flows) poorly estimated and between hydrological years, with hydrological year 2014 consistently scoring very low.

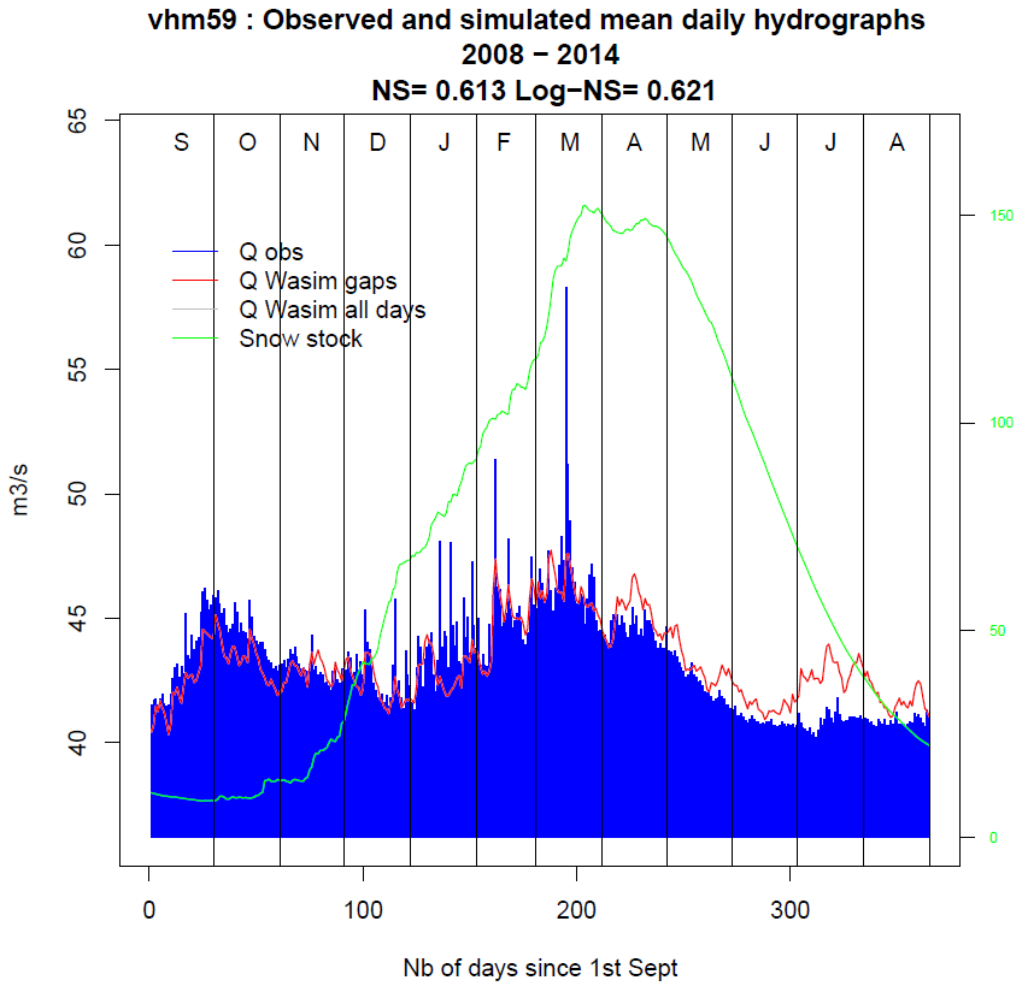

Figure 11. Mean daily discharge for the run with the highest score using the ASA optimization method.

4.2 Model validation

The validation is originally tested on hydrological years 1985 to 2016. The error measures however suggest a low performance of the model with $NS_{Qall} < 0.3$ and a strong variability of NS_{Qyear} (Figure 12). Hydrological years up to 2004 are overall badly simulated but simulation results improve after that, coinciding to the setup of new and improved gauging instrumentation at vhm 59. To allow for further analysis, it was decided to reduce the validation period to hydrological years 2004 to 2016 after the improved gauging methods had been installed.

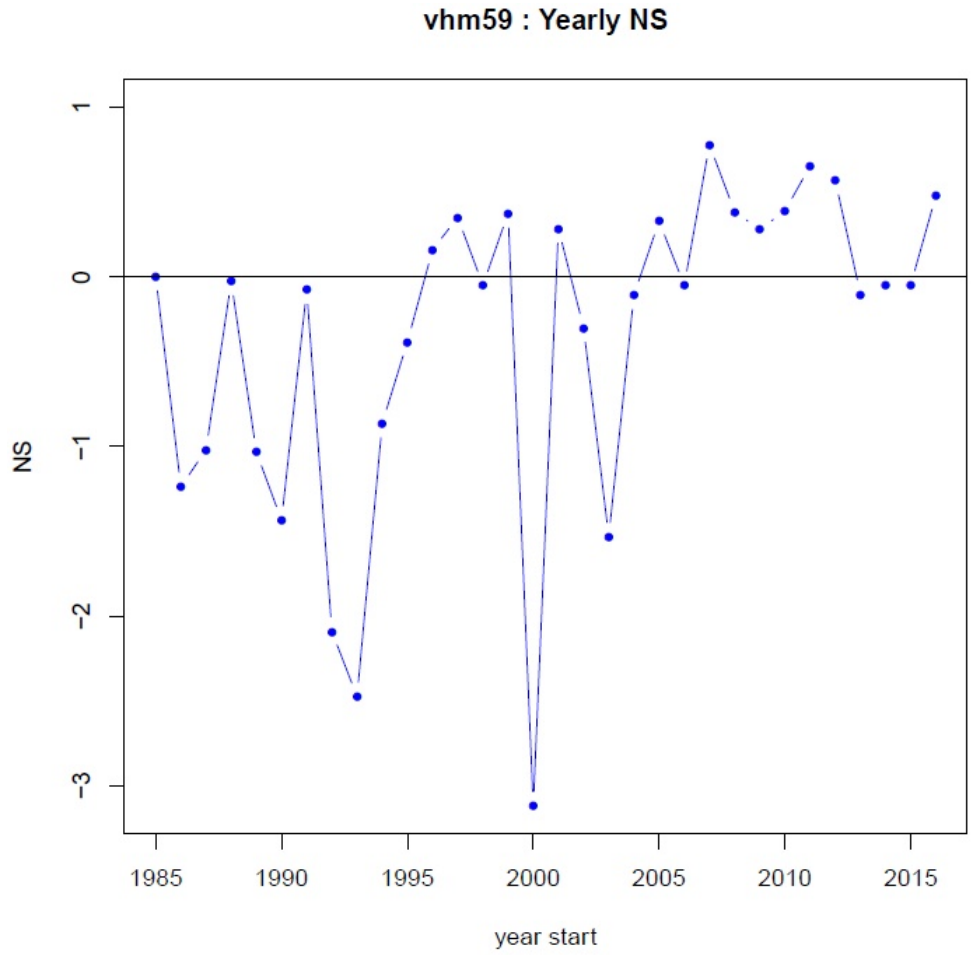

Figure 12. Efficiency criteria NS for each of the hydrological years modelled.

Table 4. Performance of five best calibration runs over the validation period (2004–2016).

	score	**NS_{all}**	**NS_{Qmax}**	**NS_{Qmean}**	**$NS_{Qspring}$**
ME_{all}	-0.82	-0.68	0.53	-0.79	-0.59
$RMSE_{all}$	4.55	4.56	6.25	4.89	4.94
NS_{Qall}	**0.487**	**0.487**	**0.033**	**0.408**	**0.397**
Log-NS_{Qall}	0.461	0.477	-0.057	0.350	0.348
ME_{Qyear}	-0.854	-0.714	0.543	-0.813	-0.602
$RMSE_{Qyear}$	**2.30**	**2.12**	**2.88**	**2.39**	**2.44**
NS_{Qyear}	0.560	0.627	0.310	0.527	0.508
ME_{Qmax}	-19.28	-18.70	-1.95	-16.40	-20.57
$RMSE_{Qmax}$	23.86	23.12	12.92	21.34	24.61
NS_{Qmax}	**-0.426**	**-0.339**	**0.582**	**-0.141**	**-0.517**
$ME_{Qspring}$	-0.59	-1.12	3.12	0.20	-0.55
$RMSE_{Qspring}$	4.81	4.89	6.96	5.38	4.11
$NS_{Qspring}$	**0.220**	**0.192**	**-0.637**	**0.023**	**0.430**
NS_{Qmean}	**0.711**	**0.639**	**0.329**	**0.741**	**0.396**
Log-NS_{Qmean}	0.725	0.654	0.317	0.747	0.367
$snowstock_{end}$	21.82	31.71	0.14	21.84	0.34

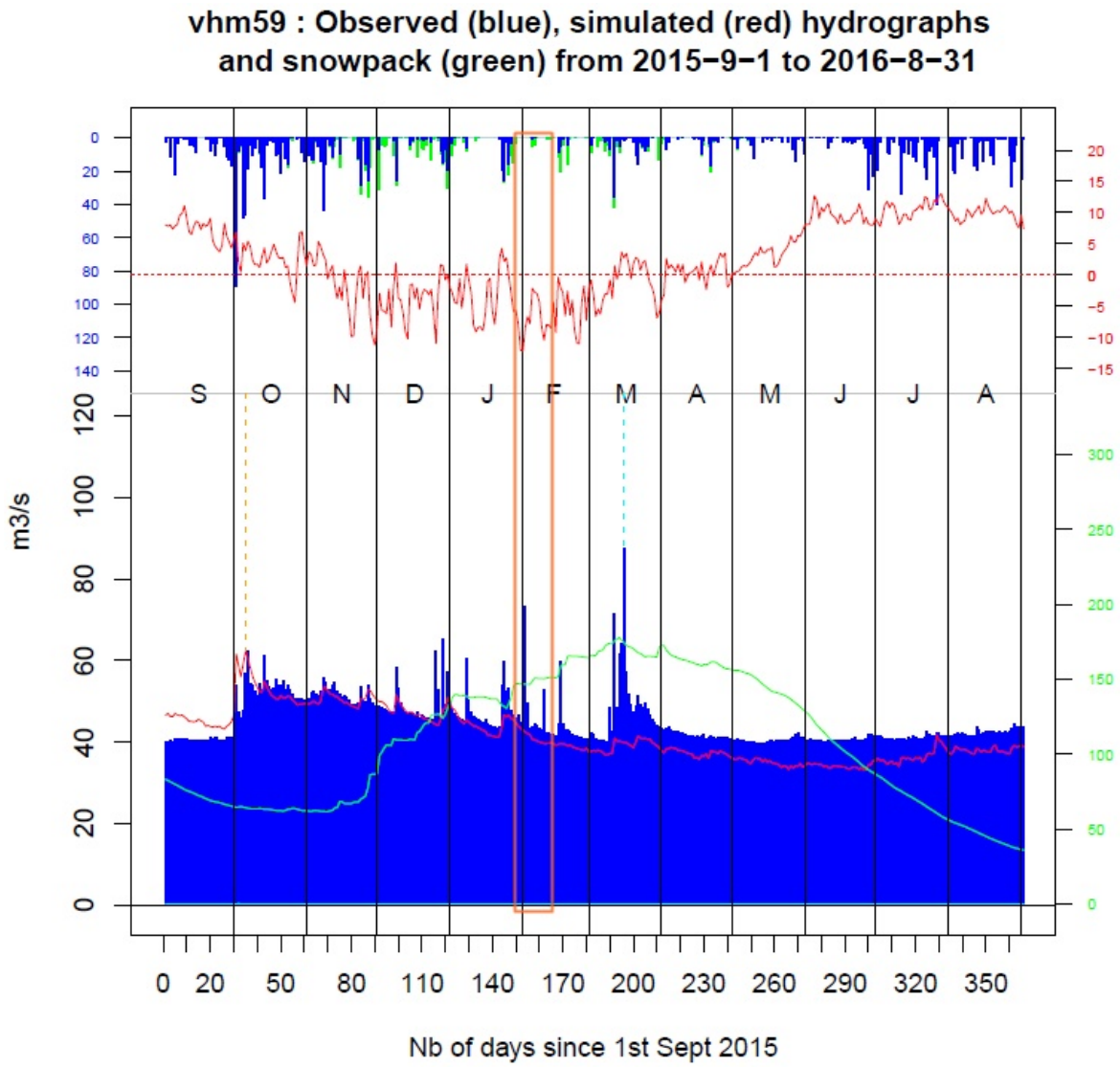

Figure 13. Example of discrepancies between the discharge and the simulation that can be explained by ice perturbation of the measurements occurring during hydrological year 2015. The orange rectangle outlines a striking ice interference event.

The statistical measures of the performance show unsurprisingly a lower NS_{Qall} for the five different setups, this can be explained in part by the fact that the data is unchecked from September 2015 to September 2017. The efficiency criterion for the daily mean (NS_{Qmean}) however is higher than in the calibration. The simulation of the annual maximum flow is low quality for the five runs. Figure 13 illustrates how ice forming on the gauge can affect the results: while the air temperatures are below -5°C and precipitations are almost null around the event, significant increases of the water level can be recorded by the meter due to the pressure of the ice cover. The model will not be able to simulate this artefact and this perturbation of the measurements is an increased source of error.

The insight provided by these error measurements shows that the model is capable of simulating the discharge in a difficult catchment.

4.3 Hydropower potential assessment

The results from the validation are used as reference for the assessment of power potential in the catchment. The discharge computed at the six different sub-catchments (Figure 9) is used to compute duration curves (APPENDIX II). To provide a better understanding of the range of discharge present, the duration curves are plotted for the five best runs, however it is recommended to consider the best score more specifically (black line) and use NS_{Qmax} solely to have a better image of the top section of the curve.

5 Discussion and conclusion

The hydrological modelling of the spring-fed river Ytri Rangá has turned out to be a greater challenge than expected, and for several reasons.

A general problem arising from modelling of the natural environment is the definition of optimal parameters. The addition of a groundwater component increased the number of parameters to be quantified. Manual and semi-automatic calibration has proven to be time-consuming and inefficient for this catchment. However, the use of the ASA automatic parameter optimization in combination with the WaSiM model has improved the quality of the results significantly.

The main unexpected challenge, however, has been to identify the quality of the observed discharge when analysing critically the performance of the model. The volcanic influence of Hekla on the catchment has resulted in a significant amount of ash deposition in the river bed, and the movement of this material affects rating-curve estimates. A combination of three updated curves was used to compute the discharge from measured water level. The measurements suggest a tendency for these curves to underestimate the discharge in May/June, while somewhat overestimating the flow from late summer to fall. This tendency is underlined by the model results consistently overestimating the flow during spring/summer while slightly underestimating it in the late summer/fall. In addition, the model validation results assert that the water level measured on a daily basis before September 2004 did not compare as well as the water level measured since 2004.

The WaSiM model is a complex hydrological model and the setting up of groundwater component involves several modules and the creation of additional grids. The validation over hydrological years 2004 to 2016, however, demonstrates that, despite the simplicity of the setup and the large uncertainties associated with unknown parameters and gauged data, the model performs well with the help of automatic optimization of the parameters. Modelling results are always to be used with a critical eye but the analysis of the results of the validation indicates that the model could be useful to estimate the water available for hydropower energy, as well as supporting the assessment of the old gauged data (before 2004) and the definition of a more comprehensive rating curve.

6 References

Arnalds, Ó. (2015). Andosols - Soils of Volcanic Regions. In *The Soils of Iceland* (pp. 47-54). Dordrecht: Springer.

Arnalds, Ó., & Óskarsson, H. (2009). Íslenskt jarðvegskort. *Náttúrufræðingurinn, 78*(3-4), 107-121.

Arsenault, R., Poulin, A., Côté, P., & Brissette, F. (2013). Comparison of stochastic optimization algorithms in hydrological model calibration. *Journal of Hydrologic Engineering, 19*(7), 1374-1384.

Bengtsson, L., Andrae, U., Aspelien, T., Batrak, Y., Calvo, J., de Rooy, W., . . . others. (2017). The HARMONIE--AROME model configuration in the ALADIN--HIRLAM NWP system. *Monthly Weather Review, 145*(5), 1919-1935.

Efstratiadis, A., & Koutsoyiannis, D. (2010). One decade of multi-objective calibration approaches in hydrological modelling: a review. *Hydrological Sciences Journal–Journal Des Sciences Hydrologiques, 55*(1), 58-78.

Einarsson, B., & Jónsson, S. (2010). *Improving groundwater representation and the parameterization of glacial melting and evapotranspiration in applications of the WaSiM hydrological model within Iceland.* Greinargerð. Reykjavík: Veðurstofa Íslands.

Goswami, M., & O'Connor, K. M. (2007). Comparative assessment of six automatic optimization techniques for calibration of a conceptual rainfall—runoff model. *Hydrological sciences journal, 52*(3), 432-449.

Gröndal, G. (2004). *Aðgreining vatnsfalla eftir rennsliháttum þeirra.* Greinargerð. Reykjavík: Orkustofnun.

Hjartarson, Á. (1994). *Vatnafarskort og Grunnvatnskorlagning.* Ritgerð til meistaragráðu. Háskóli Íslands: Reykjavík.

Hjartarson, Á. (2005). *Vatnafar við sorpstöðina að strönd í Rangárþingi Ytra.* Greinargerð, ÍSOR.

Hjartarson, Á., & Ingólfsson, Ó. (1988). Preboreal Glaciation of Southem Iceland. *Jökull*(38), 1-15.

Ingber, L. (1996). Adaptive simulated annealing (ASA): Lessons learned. *Control and Cybernetics, 25*, 33-54.

Krause, P., Boyle, D. P., & Bäse, F. (2005). Comparison of different efficiency criteria for hydrological model assessment. *Advances in Geosciences, 5,* 89-97.

Lugten, I. W. (2013). *Application of the program HydroOffice 2010 on river discharge data in Iceland.* Greinargerð. Reykjavík: Veðurstofa Íslands.

Reynisson, N. (2015). *Ytri-Rangá, Árbæjarfoss, vhm 59, V321 - Rennslislyklar 3, 4 og 5.* Greinargerð. Reykjavík: Veðurstofa Íslands.

Schulla, J. (2017). *Model Description WaSiM.* Technical report.

Seibert, J. (2000). Multi-criteria calibration of a conceptual runoff model using a genetic algorithm. *Hydrology and Earth System Sciences Discussions, 2*, 215-224.

Sigurðsson, F. (1992). Hlutur grunnvatns í vatnsafli. *Ársfundur Orkustofnunar.* Reykjavík: Orkustofnun.

Sloto, R. A., & Crouse, M. Y. (1996). *HYSEP, a computer program for streamflow hydrograph separation and analysis.* Lemoyne, Pennsylvania: US Department of the Interior, US Geological Survey.

Stefánsdóttir, G., & Egilson, D. (2014). *Vatnsformfræðilegir gæðaþættir – yfirlit yfir úrvinnslumöguleika.* Reykjavík: Veðurstofa Íslands.

Veðurstofa Íslands. (2015). *Rennslisskýrsla vatnsárið 2013/2014, V321, Ytri-Rangá, Árbæjarfoss.*

APPENDIX I Figures from the calibration best runs

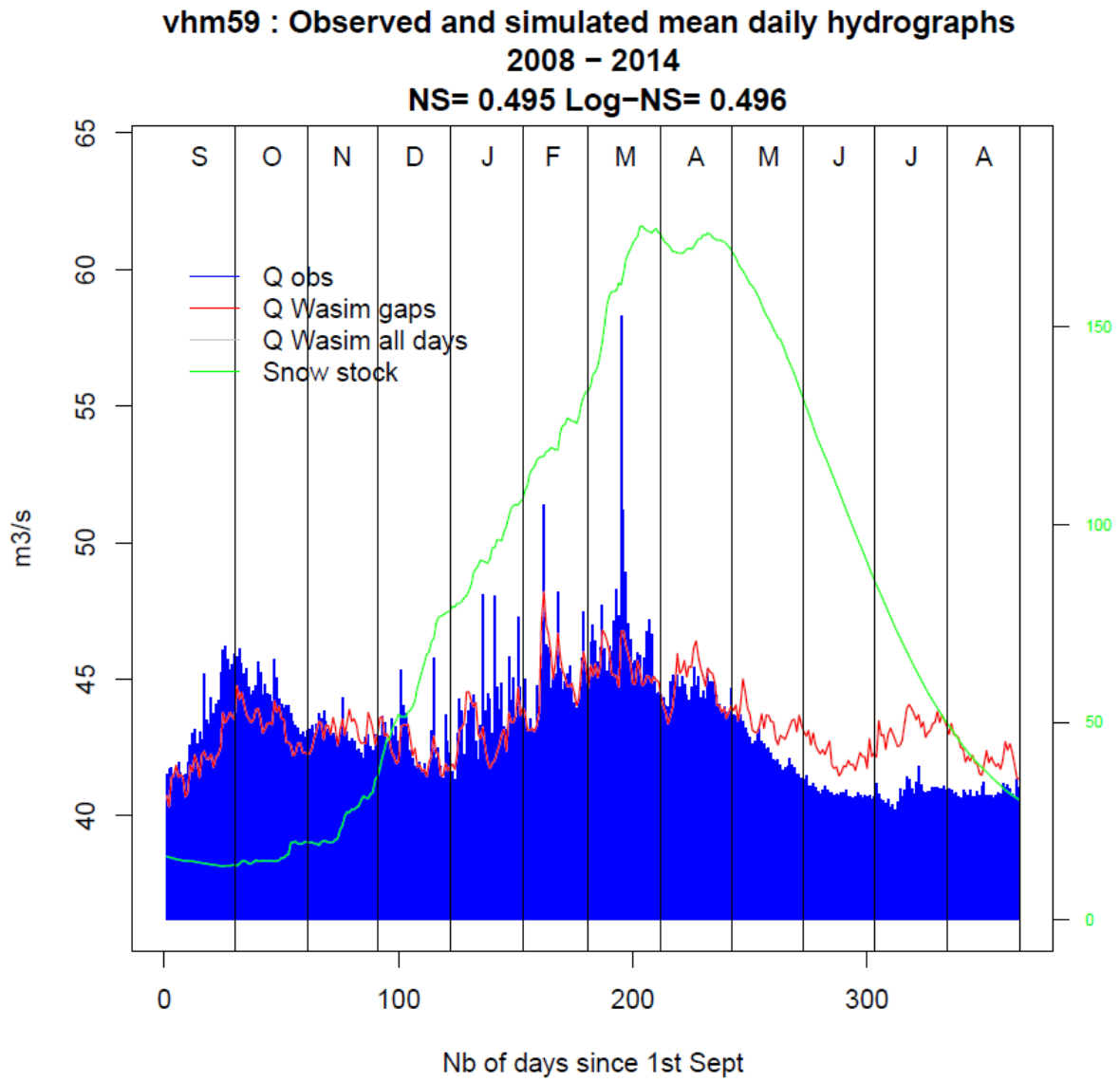

Figure A. 1. Mean daily discharge for the run with the highest NS_{Qall} using the ASA optimization method.

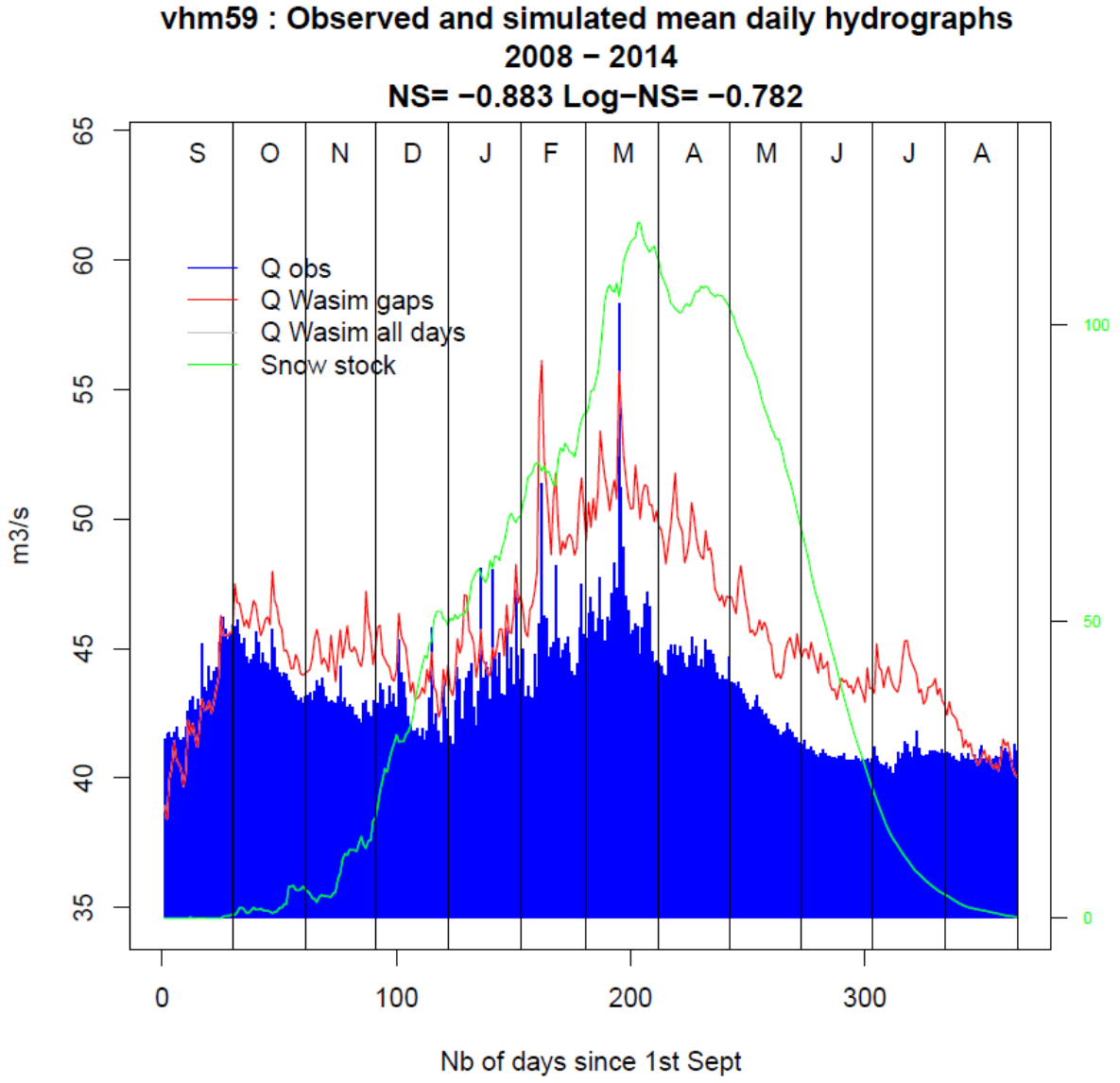

Figure A. 2. Mean daily discharge for the run with the highest NS_{Qmax} using the ASA optimization method.

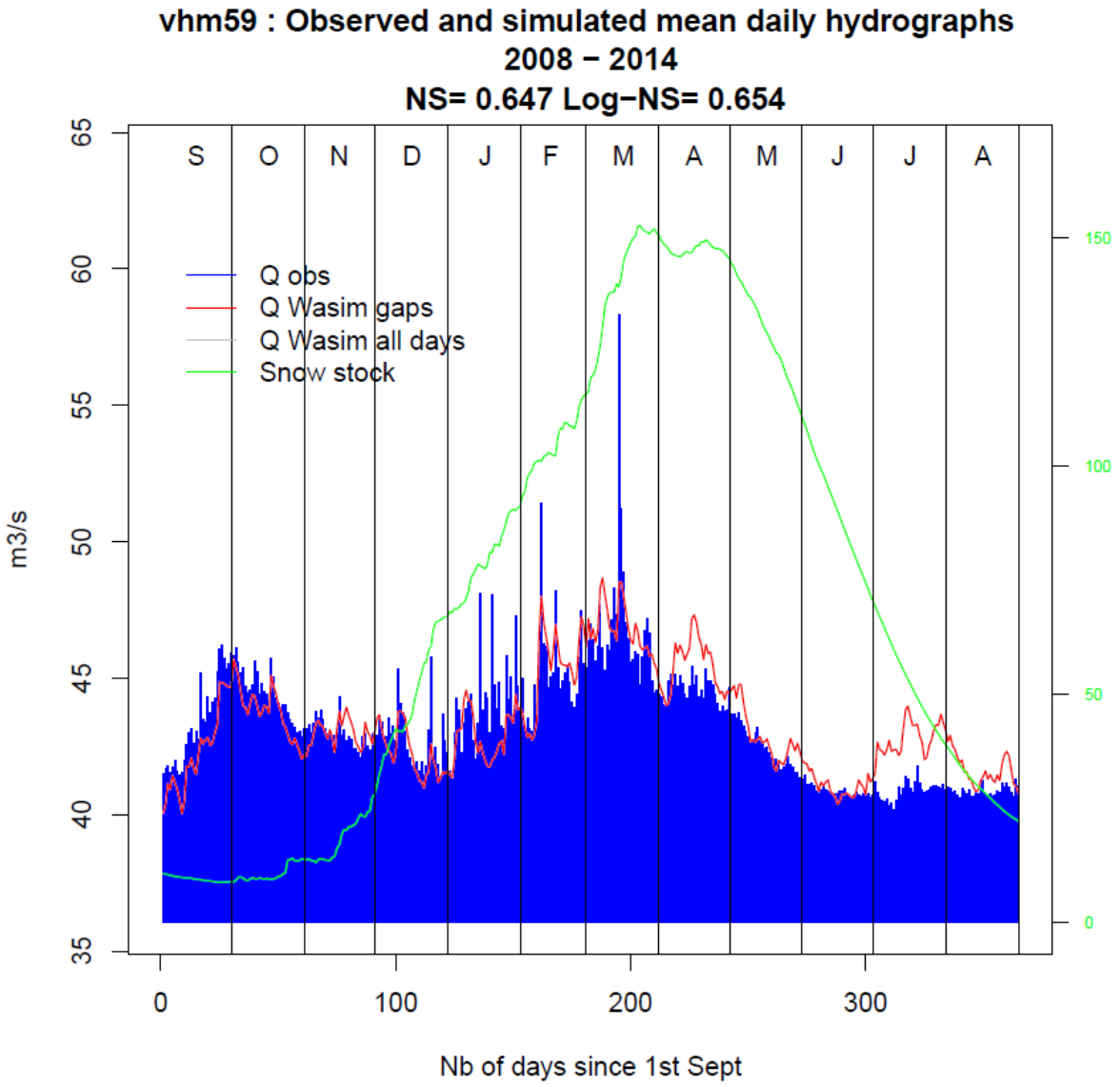

Figure A. 3. Mean daily discharge for the run with the highest NS_{Qmean} using the ASA optimization method.

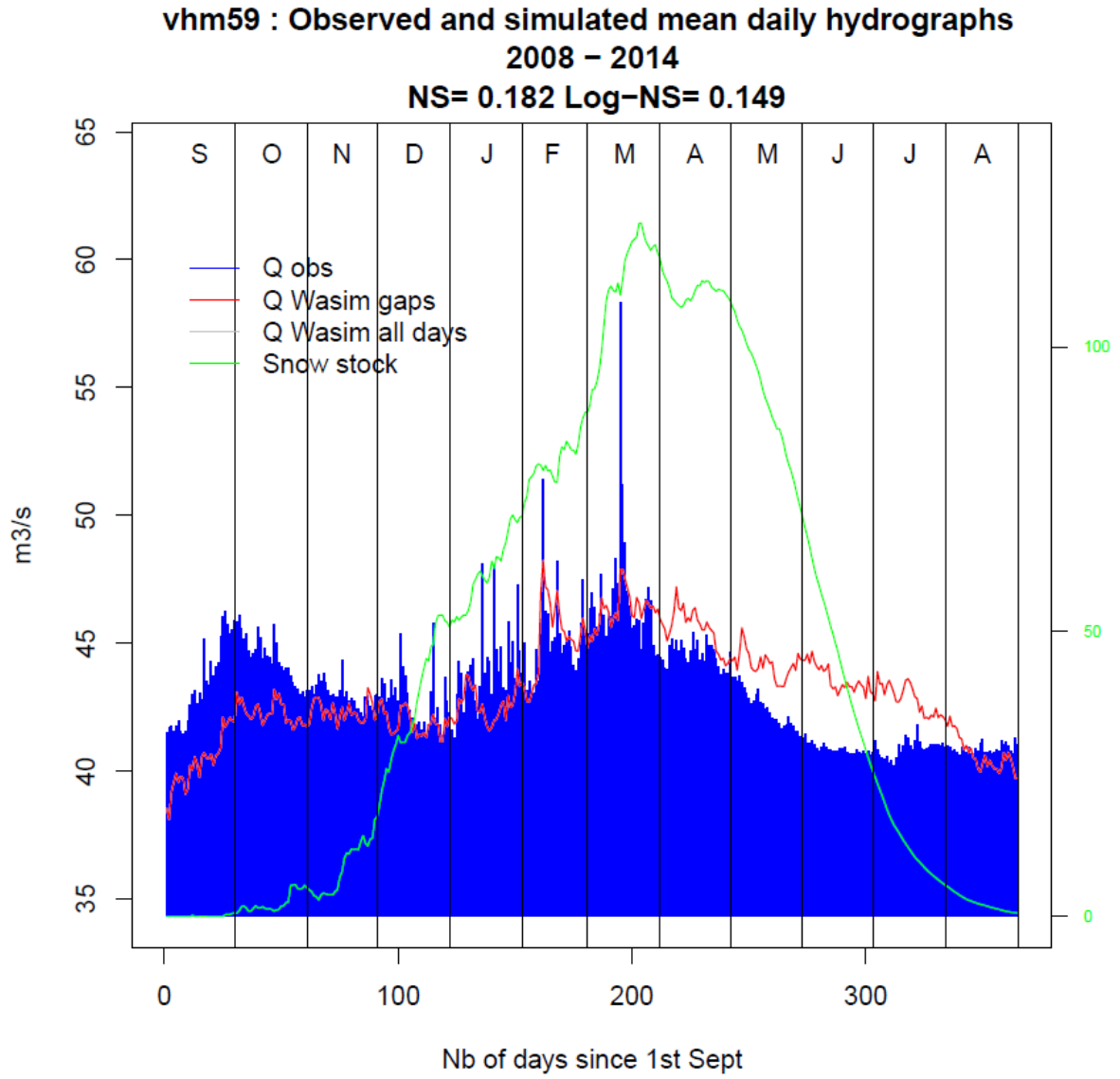

Figure A. 4. Mean daily discharge for the run with the highest $NS_{Qspring}$ using the ASA optimization method.

APPENDIX II Duration curves for the sub-catchments

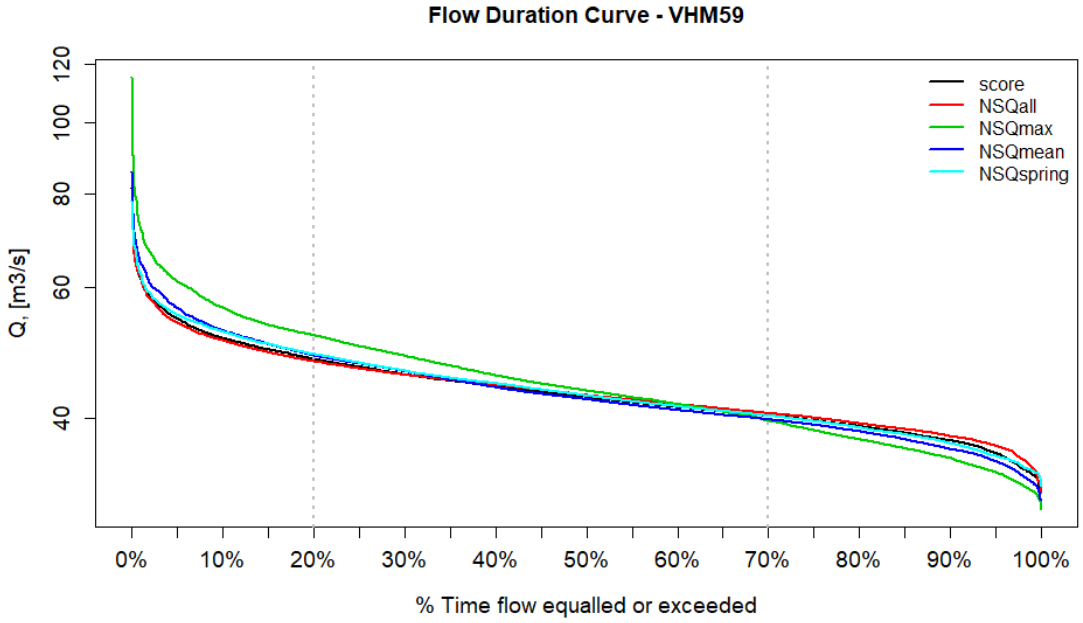

Figure A. 5. Flow duration curve at VHM 59 computed using simulated discharges over hydrological years 2004 to 2016.

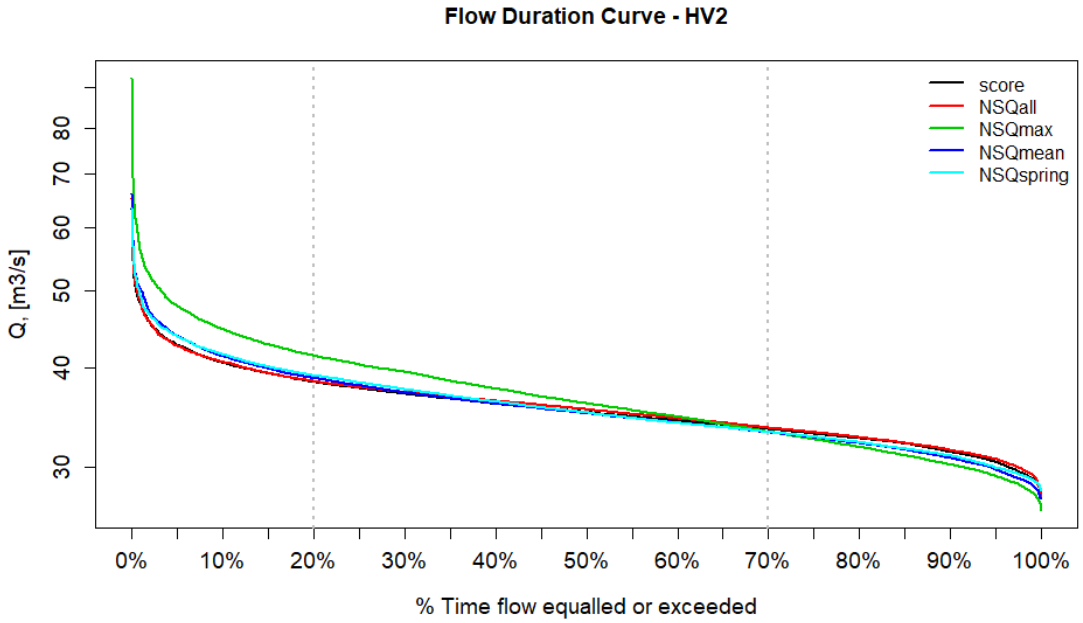

Figure A. 6. Flow duration curve at HV1 computed using simulated discharges over hydrological years 2004 to 2016.

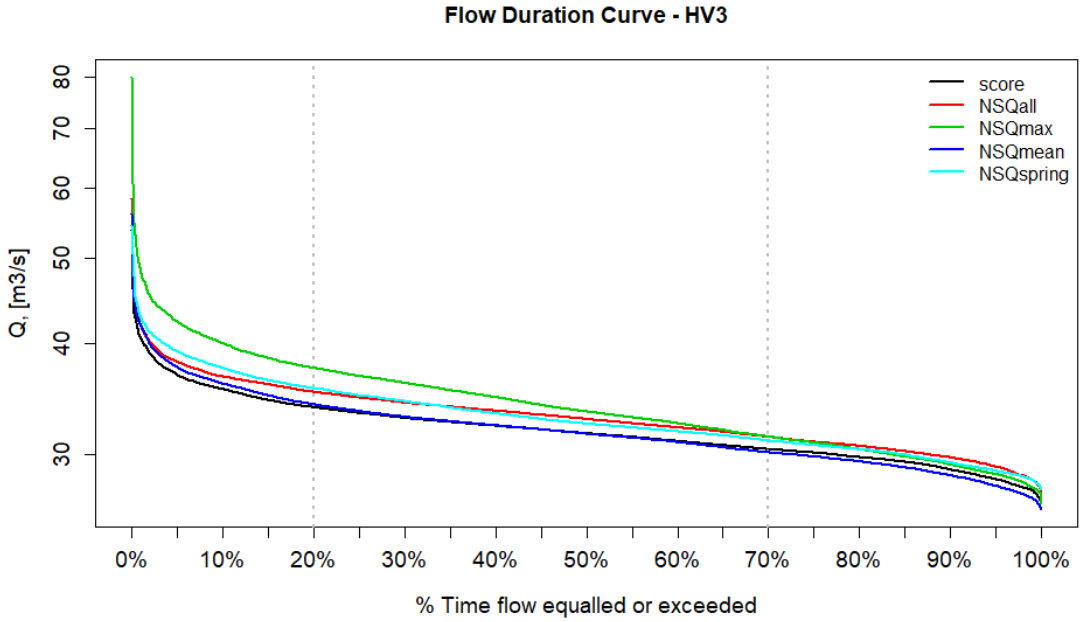

Figure A. 7. Flow duration curve at HV3 computed using simulated discharges over hydrological years 2004 to 2016.

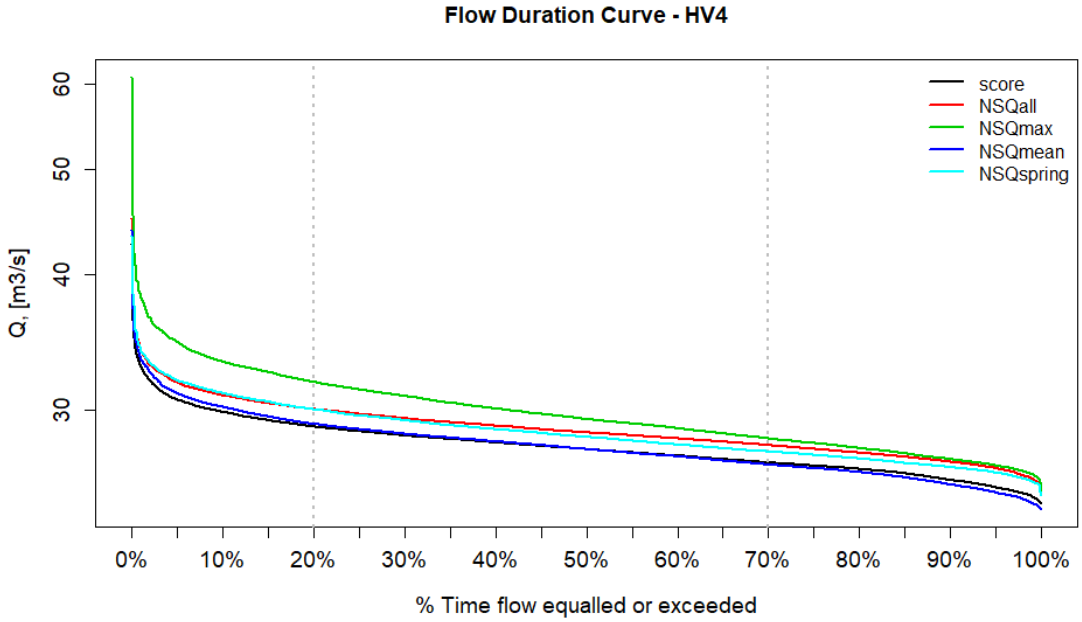

Figure A. 8. Flow duration curve at HV4 computed using simulated discharges over hydrological years 2004 to 2016.

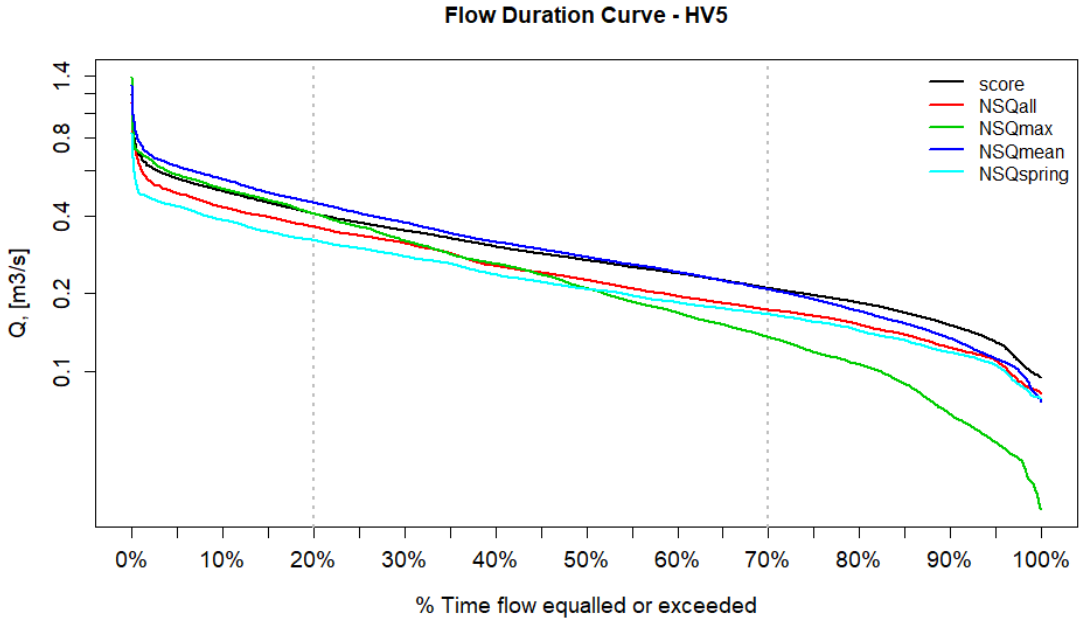

Figure A. 9. Flow duration curve at HV5 computed using simulated discharges over hydrological years 2004 to 2016.

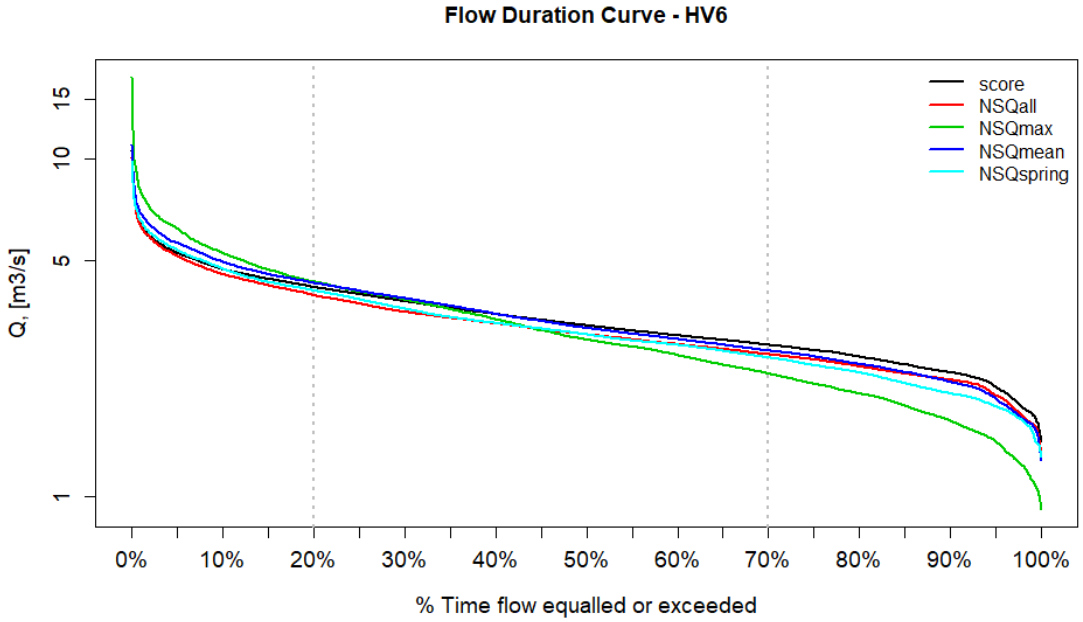

Figure A. 10. Flow duration curve at HV6 computed using simulated discharges over hydrological years 2004 to 2016.

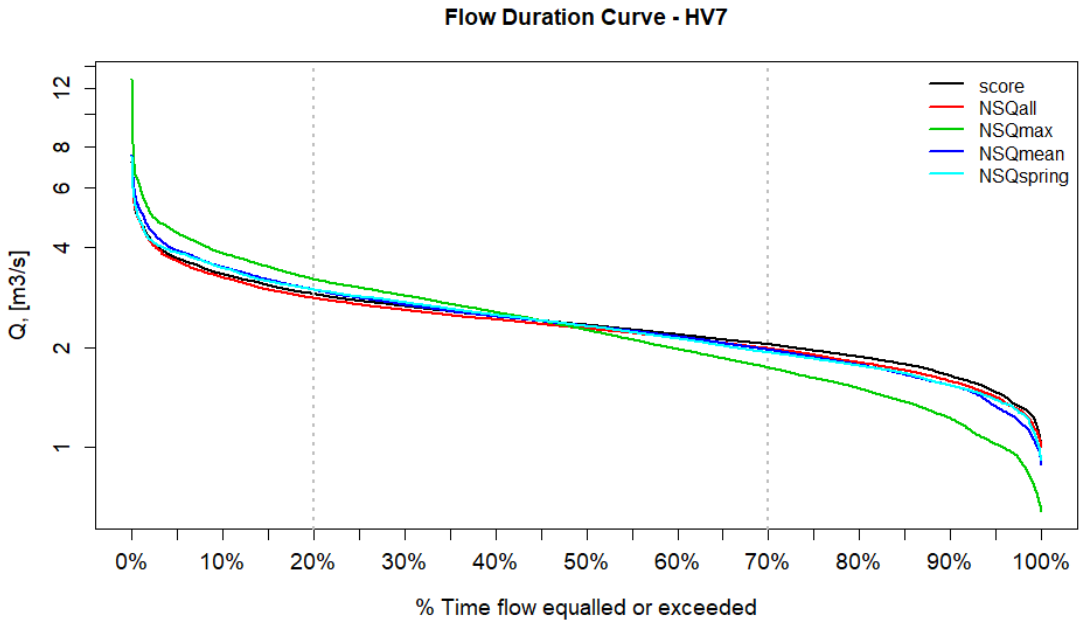

Figure A. 11. Flow duration curve at HV7 computed using simulated discharges over hydrological years 2004 to 2016.